

# An efficient hybrid biomechanical energy harvesting system using human motions for low-power applications

Mohankumar Venugopal<sup>1</sup>, Govindanayakanapalya Venkatagiriappa Jayaramaiah<sup>2</sup>

<sup>1</sup>Department of Electronics and Communication Engineering, Dr. Ambedkar Institute of Technology, Bengalore, India

<sup>2</sup>Department of Electrical and Electronics Engineering Department, Dr. Ambedkar Institute of Technology, Bengalore, India

## Article Info

### Article history:

Received Apr 16, 2022

Revised Sep 17, 2022

Accepted Sep 25, 2022

### Keywords:

Boost converter  
Electromagnetic  
Energy harvesting  
Human motions  
Piezoelectric  
Power

## ABSTRACT

The biomechanical energy harvesting system (BM-EHS) uses human daily activities to create electricity. The BM-EHS is one of the potential alternative technologies for powering wearable and implantable electronic gadgets without batteries. The hybrid BH-EHS is modeled using two different vibration source-based human activities in this manuscript. The piezoelectric (PE) and electromagnetic (EM) based EHS are combined in the hybrid BM-EHS. The PE- EHS is based on human walking and jogging motions and is represented using a mass-spring-damper system and PE stack. The EM- EHS is based on the human knee and hip motions, with shaft conversion and a DC motor. The PE, EM, and hybrid BM-based EHS are modeled using MATLAB/Simulink, and performance results are realized individually. The PE-EHS obtains the average output voltage of 0.5 V and harvests 53.18 mW of power. Similarly, the EM-EHS achieves the average load voltage of 0.567 V and 30.6 mW harvested power. The hybrid BM-EHS obtains the average load voltage of 0.79 V and harvests 86 mW of power. The proposed BM-EHS is compared with the existing EHS with better-harvested power and energy improvement for the given load conditions. Overall, the harvested power can power up the low-power applications.

*This is an open access article under the [CC BY-SA](https://creativecommons.org/licenses/by-sa/4.0/) license.*



## Corresponding Author:

Mohankumar Venugopal

Department of Electronics and Communication Engineering, Dr. Ambedkar Institute of Technology

Bengalore, India

Email: phd.mohankumar@gmail.com

## 1. INTRODUCTION

The biomechanical energy harvesting system (BM-EHS) generates electricity from daily activities. It is one of the hopeful alternative solutions to replace batteries to power the wearable and portable electronic devices. Mobile phones, computers, and laptops are portable electronic devices. These devices use battery, and the battery provides a limited amount of energy. There is always a trade-off between the battery weight, portable device power intake, and operation duration. The BM-EHS results in the power generation from daily human activities over long durations. So human power is one of the efficient energy sources. The human body parts like body heat, exhalation, blood pressure (BP), arm motion, finger motion, footfalls, and heartbeat can harvest power using an energy harvester mechanism [1], [2]. In contrast, the energy harvesting from human walking and jogging has grown tremendously. Human walking/jogging produce energy, and it is easier to harvest and convert it into electric energy with greater quality. Human walking primarily generates energy in three forms: vibrations, body inertia, and foot strike [3]. The human body's energy is available in thermal, chemical, and mechanical energy sources. To harvest power from these human body sources, there are many energy harvesting mechanisms are available, including triboelectric generator (TEG), piezo-electric

generator (PEG), electromagnetic generator (EMG), and many more [4], [5]. The PE-based EHS uses frequency up-conversion, non-linearity, harvester circuits, and spring pendulum-based methods to derive the energy from the human body parts. The PE-EHS uses the human body parts like lower limbs, human leg, walking, footwear, electronic skin, shoulder straps for energy conversion. The stretchable and Nano-crystal based PE nano-generator was recently developed in PE-based EHS. In contrast, The TE-EHS uses human wearables like shoes, wrist bracelets and human body parts like skin, cloth, arm for energy conversion. The TE-based EHS uses the ai-cushion methods, core-shell structure, flexible single-electrode, and liquid metal electrode-based methods to extract the energy from the human wearables or body parts. The flexible, Nano-crystal, cantilever, and TE fabric-based PE nano-generator was recently developed in TE-based EHS [6], [7]. The EM-EHS uses the human activities like hip movements, knees, watch, walking, arm, and a leg for energy conversion. The EM-based EHS uses the spring-clock work, springless system, non-linearity, and frequency-up-conversion-based methods to derive the energy from the human body parts. The flexible EM generator is recently developed in EM-based EHS for human activity conversion [8]–[10].

The current energy harvesting system from human motions is realized in this section with its performance analysis. Luciano *et al.* [11] present the energy harvesting system (EHS) through human knee prosthesis (HKP). The electromagnetic EHS is used to implement in HKP. The HKP model is realized to reproduce the knee motions and analyze the EHS performance. The proposed design produces the 2V voltage by consuming the 850  $\mu$ A current after walking between 7 to 30 sec. The HKP based EHS harvests the 70  $\mu$ J of energy for 2.2. k $\Omega$  of resistive load. Khalifa *et al.* [12] present human activity recognition (HAR) without using an accelerometer. The work uses different human activities for harvesting the power using HAR-based EHS. The result is compared conventional accelerometer-based HAR with HAR-based kinetic power generation model to realize the kinetic power. Niroomand and Foroughi [13] present EHS from human motion using a rotary-based electromagnetic (EM) micro-generator. The EM generator is used to convert human activities to electric energy. The micro-generator uses pendulum mechanisms with a gearbox and detects the slight vibration to produce electric Energy. The EM-based EHS delivers 416.6  $\mu$ W during normal walking for 10  $\Omega$  of resistive load. Wahbah *et al.* [14] present the vibration-based EHS from human motions using the AC-DC converter mechanism. The AC-DC converter mechanism is a PE-based EHS containing a voltage doubler and bias flip rectifier. The amount of energy harvested from the voltage doubler is 79.8 nW which is relatively more efficient than the full-bridge rectifier module. Chen *et al.* [15] introduced a knee-mounted BM-EHS with better safety and efficiency features. The BM-EHS converts mechanical source to electrical energy from human motions. The EM generator converts the bidirectional knee movements to unidirectional rotation followed by the energy extracting circuit to harvest the power. The work obtains an average power of 3.6 W for walking, sufficient to operate the portable devices.

EM generator-based respiratory effort EHS is introduced by Ali *et al.* [16], which extracts the human chest part to harvest the energy. The EM generator is wearied on the human chest, constructed using two dc motors, gear, and chest belt. The respiratory effort EHS provides 2.5 mW power to power up the EM generator's low-power devices. Ma and Liao [17] present the human gait model and its analysis using the semi-markov process (SMP). The SMP is used to extract the individual gait patterns with the help of the ground reaction forces. Around 23 subjects were considered for human gait analysis and verified the abnormal levels and phase percentages were in detail. The PE-based knee-joint EHS is designed by Kuang *et al.* [18] using a frequency-up-conversion method. The knee-joint EHS can generate the required energy to operate the wireless sensor node. The model produces 5.8 mW of average power with a lifetime of 7.3 hours. The nonlinear PE-EHS from human movements and the achievement of optimal resistance analysis are presented by Wang *et al.* [19]. Using the dominant frequency approach, the optimal resistance of the nonlinear-EHS is employed to get the greatest power. The PE-EHS from human motion is presented by Kakihara *et al.* [20]. The kinetic energy of 5 mJ is harvested using PEW materials with electric power of 0.5 mW. Qian *et al.* [21] present the PE-based footwear EHS, including heel-shaped aluminum plates with a force amplification frame. The RMS voltage of 1.08 V and 6 mW of power is obtained for 510  $\Omega$  resistive load at a walking speed of 2.5 mph. The EM-based EHS is designed with three-degree of freedom (DoF) from human body motion by Wu *et al.* [22]. The model can harvest up to 1.1 mW in walking and 2.28 mW during running.

Fan *et al.* [23] present monostable EM-EHS from human motions. The EM is designed using a magnet-spring resonator, coil, tube, and stopper. The system can harvest up to 0.5 mW of power with 4V of voltage during walking. Halim *et al.* [24] Hybrid EHS uses PE bimorph for human limb motion. The model can harvest up to 61  $\mu$ W of average power for periodic limb motion. The conventional gait models are compared with the human body model (HBM) for kinematic gain analysis by Flux *et al.* [25]. The Gain analysis for children with cerebral palsy is considered to analyze the standard deviations and P-values. Shull and Xia [26] present the wearable EHS from sliding shoes with prediction and modeling for realizing the energy rate and metabolic cost outside the lab setup. A young man with a fast-walking speed of 0.79 m/s at 0.86 Hz step frequency can harvest a power of 121 mW with 530.4 W of metabolic rate. The comparative

analysis of the cylindrical EM vibration-based EHS is presented by Pham *et al.* [27]. The work investigates EM background, coil–magnet structure, optimization methods, design parameters, implementation procedures, and performance analysis. The recent work on energy harvestings includes radio-frequency based EHS for IoT applications [28], half-duplex EHS for network security [29], vision based solar tracking system using EHS [30] and micro-electro-mechanical system (MEMS) [31].

In this manuscript, an efficient hybrid bio-mechanical energy harvesting system from different human motions is modeled and analyzed its performance metrics. The proposed hybrid BM-EHS model can harvest more power and energy than individual PH/EM-based EHS. The performance results of the hybrid work are suitable for low-power applications, especially wireless sensor nodes. The manuscript's organization is summarized as follows: The proposed BM-EHS module is explained in detail with the PE and EM modules in section 2. The results and discussion, including simulation results, performance, and comparison tabulation of the proposed work, are highlighted in section 3. The overall work with performance improvement with the futuristic scope is mentioned in section 4.

## 2. HYBRID ENERGY HARVESTING SYSTEM

The hybrid biomechanical energy harvesting (BMEH) system is represented in Figure 1. The BMEH system mainly contains two vibration sources, energy conversion modules, AC to DC Rectifiers, Boost converter with a control mechanism, load, and battery model. In this work, two different types of vibration sources are considered: i) human walking/jogging data (leg and foot) as a first source and ii) human knee movement/hip movement data (both left and right). The first vibration source data (acceleration) is converted to electric energy using a mass-spring-damper module and the PE stack actuator. The second vibration source data (angle) is converted to electric energy using an electromagnetic system with DC motor. The PE stack and DC motor data values are voltages connected to the AC to DC rectifiers individually. The boost converter (BC) receives the rectified DC voltages in series and performs the control mechanism to boost the DC Values using a PI controller. The BC output voltage connects to the battery model via load. The BC converter output provides the output voltage and extracted power. The battery model maintains the nominal battery voltage based on harvesting by increasing the start of charge (SoC) and discharging the current. A hybrid combination of vibration sources may gather more power and energy than a single source. The detailed illustration of the model is explained in the following subsections. The vibration-source-1 and source-2 data set are collected from the different human activities [32], [33] and used further in BM-EHS model. The QP20W Piezo sensor film specifications [34] are considered for the PE Stack actuator. The C23 series-based DC motor [35] specification is considered for the DC motor model. The BM-EHS model is configurable to any PE sensor film and DC motor specifications.

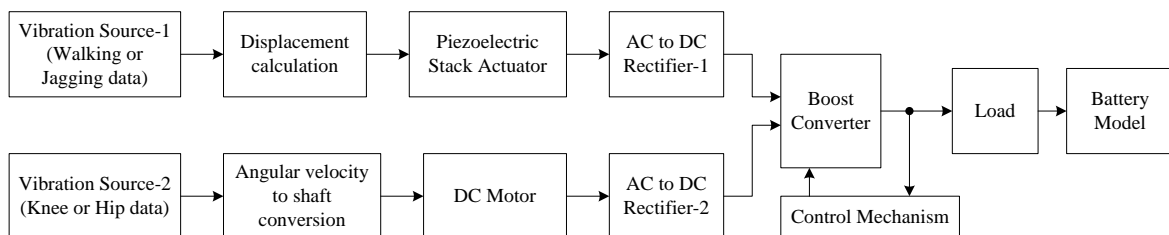


Figure 1. Proposed hybrid bio-mechanical energy harvesting system (BM-EHS)

### 2.1. Piezo-electric based EH system

The PE energy harvesting is performed using a mass-spring-damping system and Piezo stack for human motions. The triaxial acceleration dataset is collected from reference [32] using human activities like normal walking (leg and foot) and jogging (leg and foot). The PE harvester obtains the resonant frequency of 2.0751 Hz using proof mass ( $m$ ), damping factor ( $b$ ), and spring-constant ( $k$ ). The overall magnitude of the acceleration is calculated using (1) [33].

$$a(t) = \sqrt{a_x(t)^2 + a_y(t)^2 + a_z(t)^2} \quad (1)$$

Where  $a_x(t)$ ,  $a_y(t)$ , and  $a_z(t)$  are sensed data from an accelerometer of the corresponding x, y, and z axes. The calculated raw accelerometer data contains constant component values due to earth gravity, which has to be filtered out using the filter technique. The raw accelerated information is filtered using 3<sup>rd</sup> order

Butterworth filter (high-pass) with a cut-off frequency of 0.1 Hz. Apply the Laplace transformation function for the filtered data to the conversion of the proof mass displacement, and it is represented in (2) [33].

$$z(t) = L^{-1}\{Z(s)\} = \frac{A(s)}{s^2 + \frac{b}{m}s + \frac{k}{m}} \quad (2)$$

Where  $Z(s)$  and  $A(s)$  are Laplace transformation of the proof mass displacement  $z(t)$  and magnitude of the acceleration  $a(t)$ ,  $m$  is proof mass,  $b$  is damping factor, and  $k$  is spring constant.  $Z_L$  limits the proof mass displacement  $z(t)$  result, represented in Figure 2. The proof mass displacement data is considered an ideal force source and applied to the piezoelectric stack actuator. The actuator changes the mechanical force to electric energy using Piezo materials. The direct and indirect piezoelectric effect is represented in (3) and (4) [36].

$$E_d = c\sigma + \epsilon \cdot E_i \quad (3)$$

$$\varepsilon = s\sigma + cE_i \quad (4)$$

$E_d$  and  $E_i$  are electric displacement and field intensity respectively,  $c$  is PE coefficient,  $\sigma$  is stress constant,  $\epsilon$  permittivity,  $s$  is elastic compliance, and  $\varepsilon$  is strain constant. In (3) represents the direct effect of the PE and converts the mechanical force to electrical energy using PE materials. In (4) represents the indirect effect of the PE and converts the electrical signal to mechanical energy. The PE stack actuator is connected with a voltage sensor to produce the PE voltage ( $V_{pe}$ ).

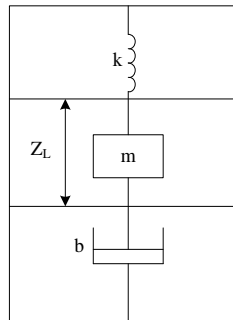


Figure 2. Mass-spring-damper system

The vibration source-1 (human motion) conversion results are represented in Figure 3. The triaxial accelerometer input data for jogging (leg) and jogging (foot) is shown in Figures 3(a) and 3(b). The raw accelerated data is filtered using a high-pass filter. So filtered acceleration data for jogging (leg) and jogging (foot) is shown in Figures 3(c) and 3(d). The proof mass displacement results for jogging (leg) and jogging (foot) are calculated using (2), and it is depicted in Figures 3(e) and 3(f), respectively.

## 2.2. Electromagnetic based EH system

The electromagnetic energy harvesting (EMEH) system converts mechanical torque to electrical energy from human motions (knee and hip movements). The vibration source contains angle values from the knee or hip movements from human activities. The EM conversion mechanism mainly includes angular velocity source rotational spring, gearbox, and DC motor [37]. The angular velocity source generates the velocity differential and produces the mechanical rotational conversion through the angle values. With positive torque, the rotational spring is connected with angular velocity for mechanical rotational transformation. The gearbox receives the angular velocity as the input shaft and generates the output shaft. The gearbox also maintains the torque in a positive direction. The DC motor converts the mechanical values from the torque to electric values. The direction of DC motor can be changed by shifting the torque or back-emf constants. In general, the voltage drops across the resistance ( $R$ ) and back emf is represented in (5).

$$V_{em} = \frac{T}{k_T} \cdot R + k_E \cdot \omega \quad (5)$$

Where ‘T’ is torque,  $k_T$  and  $k_E$  are torque and electric constant, inherent to the DC motor,  $\omega$  is the angular velocity, ‘R’ is resistance. The back emf is a product of the angular velocity and electric constant. The current supplied to the motor is proportional to the motor’s torque ( $I = T / k_T$ ). The maximum torque (Speed) occurs when the angular velocity is zero. The angle values for EM-EHS is represented in Figure 4. It has angle values of knee (left) data in Figure 4(a) and hip data (left) in Figure 4(b). The vibration sources summary is tabulated in Table 1. The average magnitude of the acceleration data (m/s.s) from the human motions like walking and jogging (leg and foot) is used further in PE-EH. The average angle values from human activities like knee and hip movements (left and right) are used further in EM-EH. The PE and EM voltages from the corresponding human motions are tabulated in Table 1 and are used further for the energy harvesting process. The magnitude of acceleration and PE voltages are derived from the (1) and (2). The average of the angles and EM voltages are generated using on EM-EH module.

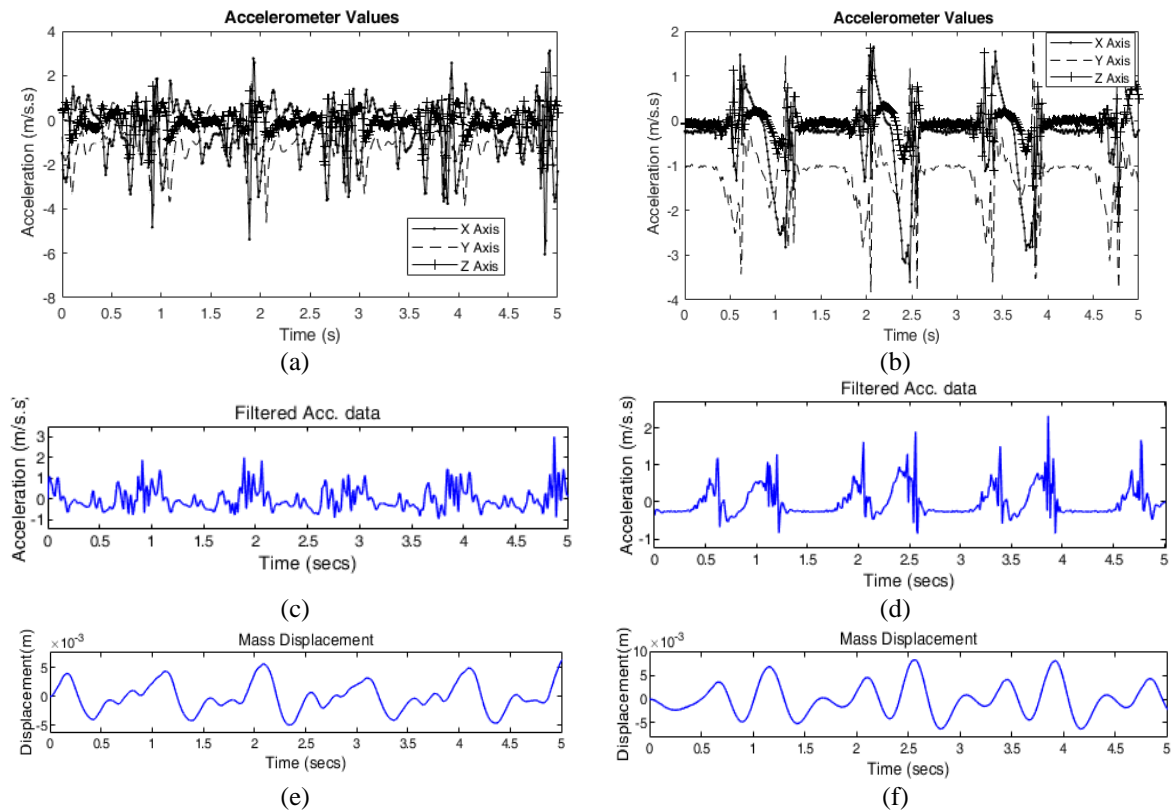


Figure 3. Vibration source-1 (human motion) conversion results, (a) accelerometer input for jogging (leg), (b) accelerometer input for jogging (foot), (c) filtered acc, data for jogging (leg), (d) filtered acc. data for jogging (foot), (e) mass displacement results for jogging (leg) and (f) mass displacement results for jogging (foot)

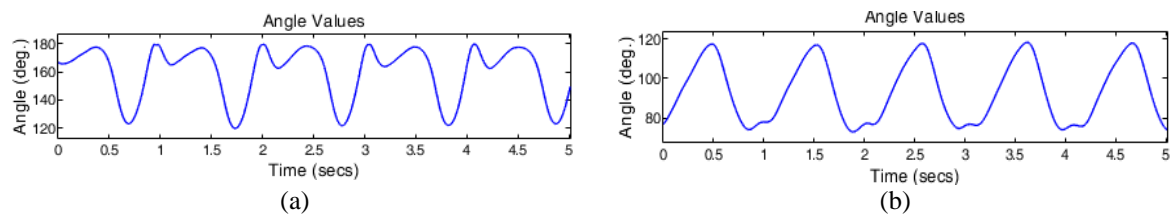


Figure 4. Angle values of the knee and hip data (a) angle values of knee (left) and (b) angle values of hip (left)

Table 1. Summary of the vibration sources

Human Motions	Mag. of Acc (m/s.s)	PE Voltage (V)	Human motions	Avg. of angle	EM Voltage (V)
Normal walk (leg)	1.399	0.8586	Knee (left)	160.6957	0.0579
jogging (leg)	1.7525	0.783	Knee (Right)	161.209	0.1162
Normal walk (foot)	1.085	0.8676	Hip (Left)	93.473	0.0131
jogging (foot)	1.5687	0.8939	Hip (Right)	90.523	0.0463

### 2.3. AC to DC rectifier

The PE and EM voltages connected individually to the full-wave bridge AC to DC rectifiers. The rectifier uses four rectifying diodes connected in a closed-loop manner (bridge) to generate the desired DC voltage. The AC- to DC rectifier model is represented in Figure 5. A pair of diodes conducts during each half cycle. During the positive half cycle of the supply voltage, the upper left diodes and lower right-side diodes are connected in series, and the remaining two diodes are reverse biased. During the negative half cycle of the supply voltage, the lower left side diodes and upper right-side diodes are connected in series, and the remaining two diodes are reverse biased and are "OFF". The smooth capacitor ( $C_r$ ) is connected across the load resistance and converts the full-wave rippled output into smooth DC voltage output ( $V_r$ ). In Hybrid BM-EHS, the two rectifier outputs are connected in series, which doubles the rectifier voltages to improve the harvesting system. However, the corresponding internal resistance is associated across voltage terminals, which reduces the rectifier voltage up to 30%.

### 2.4. Boost converter

The Boost converter model with a controller is represented in Figure 6. The boost converter (BC) enhances the input voltage to the desired level. The typical boost converter (DC to DC) mainly contains the inductor, MOSFET switch, diode, capacitor, resistor, PI controller, and PWM generator. The rectified voltage acts as an input source and is connected to the inductor ( $L_b$ ). The MOSFET acts as the switch is connected to the rectified voltage. The diode acts as a second switch connected to the capacitor ( $C_b$ ) and resistor ( $R_b$ ) in parallel. The rectified voltage is connected with an inductor to produce the constant input current. The MOSFET switch is controlled using a PI controller, and it can be turned on and turned off using pulse width modulation (PWM). The PWM generator (DC to DC) produces the gate pulses at a switching frequency of 10 kHz to the PI controller's switch. When the switch is "OFF," and the diode is "ON," then the polarity of the inductor is changed. The inductor discharges the stored energy and dissipates at the resistor to maintain the current flow in the same direction. The voltage developed across the resistor is BC voltage ( $V_b$ ).

The BC voltage is linked to an inductor and a DC voltage across the load resistance to create the load voltage. The battery inductor across the load stores the energy. The inductor produces the battery current, followed by the DC voltage from the battery. The battery current will be positive when charging, and the battery current will decrease when discharging.

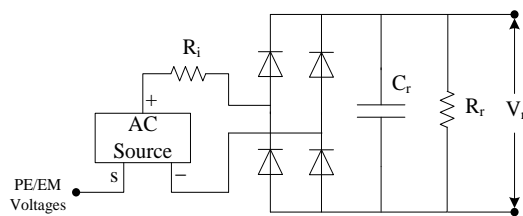


Figure 5. AC- to DC rectifier model

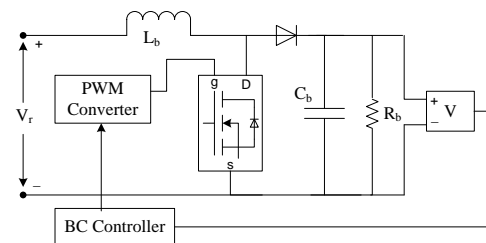


Figure 6. Boost converter model with controller

## 3. RESULTS AND DISCUSSION

The hybrid BM- EHS using MATLAB/Simulink, represented in Figure 7. The model mainly has two different vibration sources: mechanical to electrical conversion models, AC to DC rectifiers, boost converter, and battery and load for wireless sensor node applications. The human motion-based two vibration sources are converted from mechanical to electrical energy using PE stack and electromagnetic generator (DC motor). The full-wave rectifier converts the AC to smoothed DC voltage. The boost converter boosts the DC input to the desired DC voltage using the control mechanism. The BC converter outputs provide voltage and current to estimate the harvested power and energy. The load resistance is connected across the battery to calculate the battery voltage after harvesting. The specification of the hybrid BM-EHS model is tabulated in Table 2 with parameters and its values.

The PE and EM voltages simulation results are represented in Figure 8 based on corresponding vibration sources. The PE voltages for jogging (leg and foot) is depicted in Figures 8(a) and 8(b). The average PE voltage of normal walking (leg and foot) is 0.8586 V and 0.8676 V. Similarly, the average PE voltages of 0.783 V and 0.8939 V are obtained for jogging (leg) and jogging (foot). The EM voltages for knee and hip movement (left) are shown in Figures 8(c) and 8(d). The average EM voltage of knee movement (left and right)

is 0.0579 V and 0.1162 V, respectively. Similarly, the average EM voltages of 0.0131 V and 0.0463 V are obtained for hip movement (left and right). The average DC motor power is varied from 44 to 46  $\mu$ W for knee movement and 11 to 15  $\mu$ W for hip movement.

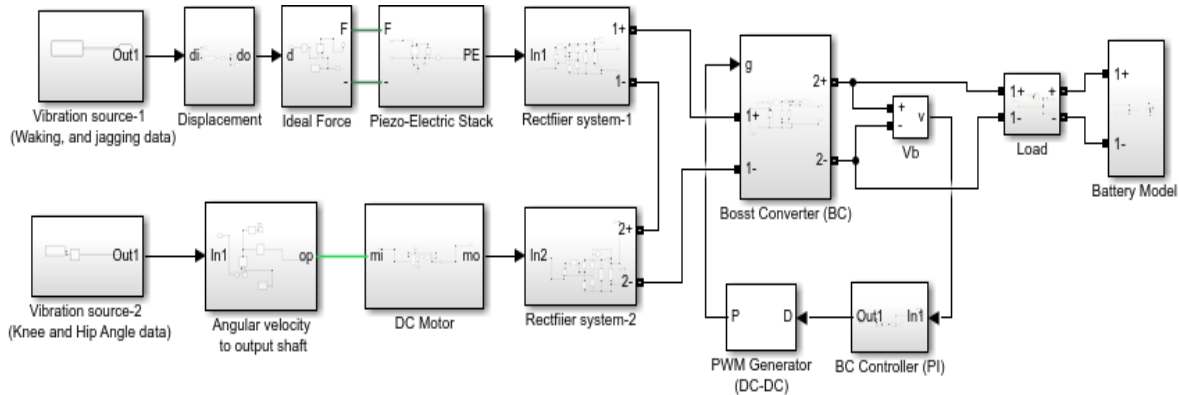


Figure 7. Hybrid bio-mechanical EHS Simulink model

Table 2. Parameters and its values used in hybrid BM-EH system

Parameters	Component Names	Values
Vibration conversion and Piezoelectric Stacked actuator parameters	Proof Mass (m), Spring constant (k), Spring damping factor	$10^{-3}$ Kg, 0.17 Kg.s <sup>2</sup> , 0.0055 Kg/s
	Stack Area, Piezo layer Thickness, Number of layers	1518.06 mm <sup>2</sup> , 45.97 mm, 3
	PE charge constant, Dielectric constant, Elastic Compliance	23 m/V, 12 F/m, 330 m <sup>2</sup> /N
Electro-magnetic + DC Motor parameters	Spring Rate, Gear Ratio	10 Nm/rad, 5
	Armature resistance and inductance	0.60 $\Omega$ , 0.35 mH
	Back-EMF Constant	0.0191 V/(rad/s)
Rectifier and Boost converter parameters	Rotor Inertia, Rotor damping, Initial rotor speed	155.4 g.cm <sup>2</sup> , 1 Nm/(rad/s), 4700 Rpm
	Diode resistance, Forward voltage	0.001 $\Omega$ , 0.7V
	Rectifier capacitance and resistance	10 $\mu$ F, 100 $\Omega$
Battery specifications	BC inductance, Capacitance, resistance	100 $\mu$ H, 10 $\mu$ F, 100 $\Omega$
	Switching frequency for PWM generation	10 kHz
	Battery Used	Lithium-Ion
	Nominal Voltage (V), Rated Capacity (Ah),	1 V, 1 Ah
	Initial SoC (%), Battery Response time (sec), Load resistance	50%, 1sec, 100 $\Omega$

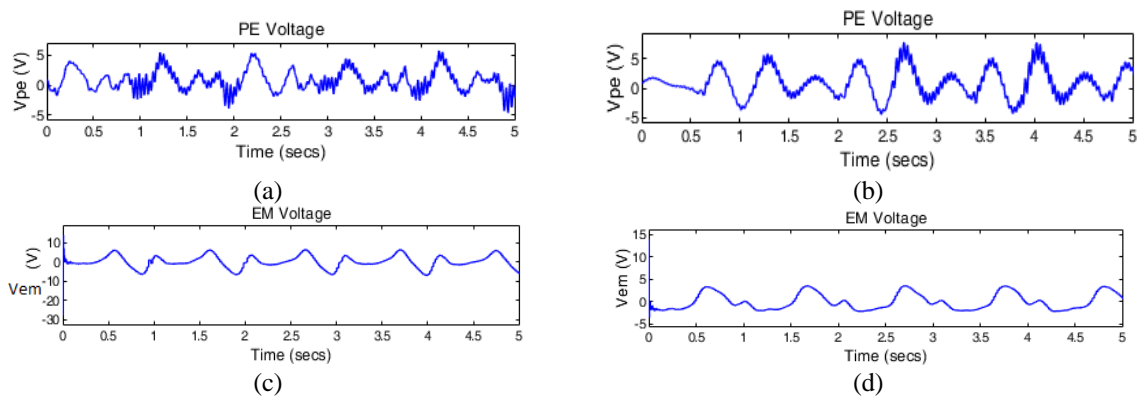


Figure 8. Simulation results of PE and EM voltages: (a) PE voltage of jogging (leg), (b) PE voltage of jogging (foot), (c) EM voltage of knee (left) and (d) EM voltage of hip (left)

The simulated results of the boost converter voltages (input and output) are illustrated in Figure 9. The BC voltages of the jogging (leg) + knee (left) and jogging (leg) + hip (left) is shown in Figures 9(a) and 9(b).

The BC boosts the input voltage and obtains the smooth required output voltage. The average of the BC output voltage is greater than the BC input voltage.

The results of the harvested power of hybrid BM-EHS is illustrated in Figure 10. The jogging (leg) + knee (left) in Figure 10(a) and jogging (leg) + hip (left) data set is depicted in Figure 10(b). The harvested power is calculated based on BC output voltage and current. The average harvested power for jogging (leg) + knee (left) data is 111.3 mW and 34.9 mW for jogging (leg) + hip (left) data.

The battery model results for hybrid BM-EHS is shown in Figure 11. The battery current in Figure 11(a) and SoC (%) shown in Figure 11(b) for the jogging (leg) + knee (left) hybrid data. The lithium-Ion battery is selected with a nominal voltage of 1 V by considering the initial SoC of 50% with 1 sec of battery response time. The battery current starts discharging afterload resistance connected to the battery. The SoC starts increasing up to 50.006 % by maintaining the battery voltage of 1.07 V.

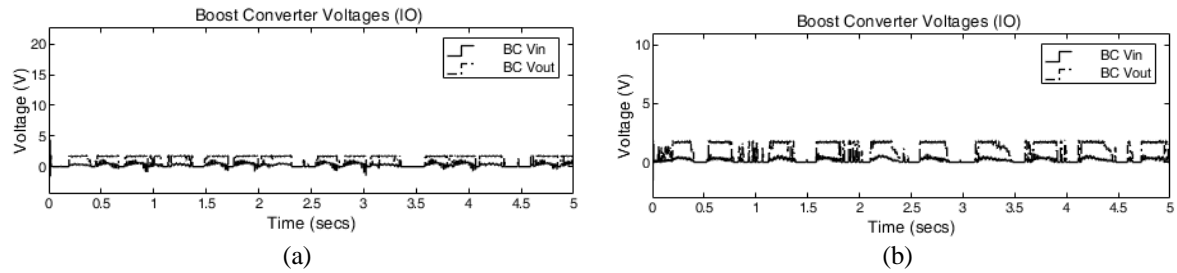


Figure 9. Simulation results of the boost converter: (a) jogging (leg) + knee (left) and (b) jogging (leg) + hip (left)

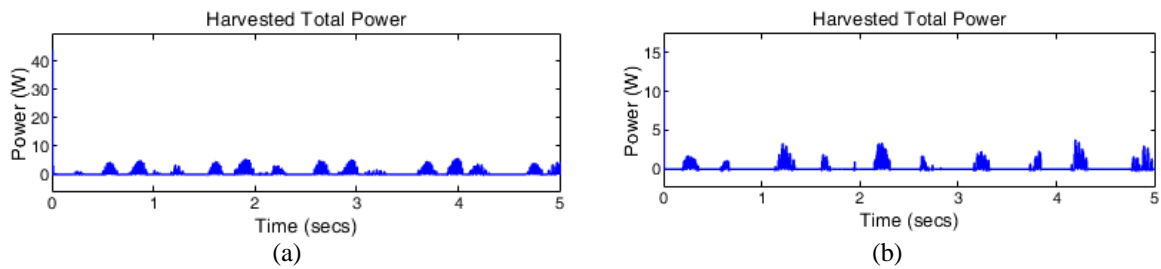


Figure 10. Harvested power of Hybrid BM-EHS: (a) jogging (leg) + knee (left) and (b) jogging (leg) + hip (left)

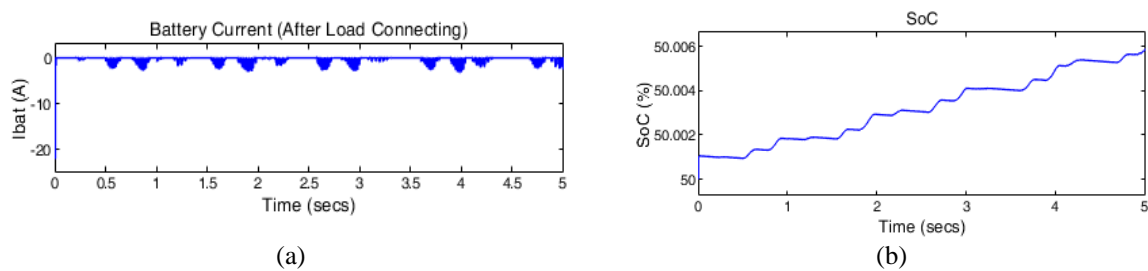


Figure 11. Battery model results for Hybrid BM-EHS: (a) battery current and (b) SoC

The summary of output voltage levels (V) and derived power (mW) results for different human motions is illustrated in Table 3. The energy harvester type, human activity, and its identification (ID) for output voltage and extracted power are shown in Table 3. The average output voltage and harvested power in PE-EHS are 0.50 V and 53.17 mW respectively. Similarly, in EM-EHS, 0.568 V and 30.6 mW of average output voltage and harvested power are obtained. The average output voltage of 0.793 V and average harvested power of 87 mW are obtained in hybrid BM-EHS. The hybrid BM-EHS provides better output voltages of 42 % and 28.3 % than PE-EHS and EM-EHS. Similarly, the hybrid BM-EHS provides better average harvested power of 37.9 % and 64.3 % than PE-EHS and EM-EHS, respectively.



**Table 3. Summary of load voltage and harvested power results for different human motions**

Energy harvester Type	Input ID	Human motions	Output voltages (V)	Harvested power (mW)
Piezo-electric (PE)	A1	Normal Walk (Leg)	0.5883	45.9
	A2	Jogging (Leg)	0.494	49.8
	B1	Normal Walk (Foot)	0.0191	19.3
	B2	Jogging (Foot)	0.7325	97.7
Electromagnetic (EM)	C1	Knee (left)	0.7477	56.6
	C2	Knee (right)	0.7695	51.6
	D1	Hip (left)	0.4406	9.4
	D2	Hip (Right)	0.3122	4.8
Hybrid (PE + EM)	A2 + C1	Jogging (Leg) + Knee (Left)	0.9048	111.3
	B2 + C1	Jogging (foot) + Knee (Left)	0.9535	140
	A2 + D1	Jogging (Leg) + Hip (Left)	0.5683	34.9
	B2 + D1	Jogging (foot) + Hip (Left)	0.7442	61.4

The graphical representation of the average harvested power and energy for different human motions is shown in Figure 12. The obtained harvested power or energy is suitable to power up any portable devices and WSN applications. The average harvested energy is 124.2 mJ, 80.5 mJ, and 222.2 mJ is obtained for PH-EHS, EM-EHS, and hybrid BM-EHS, respectively. The graphical representation of the output voltages and battery voltage after harvesting for different human motions is shown in Figure 13. The hybrid combination of jogging (foot) + knee (left) data set provides better output voltage and harvested power than other hybrid combinations. The output voltage is supplied to the battery model after harvesting. When the load is connected to the battery, the battery model maintains the average battery voltage of 1.07 V using harvested energy.

The performance comparison of the proposed BM-EHS with the existing EHS is tabulated in Table 4. The vibration source, energy harvesting type, obtained output voltage, power, and energy for the given load resistance are considered for comparison. The existing EHS works are discussed in earlier section 2. The obtained output voltages are varied from 0.1 V to 2 V from these harvester systems. The harvested power and energy are varied up to 60 mW and 150 mJ, respectively, based on the internal harvester architecture and vibration data for the given load conditions. The values are from these energy harvester systems are acceptable and suitable in low-power applications. The proposed designs harvest more power and energy than the other existing EHS modules.

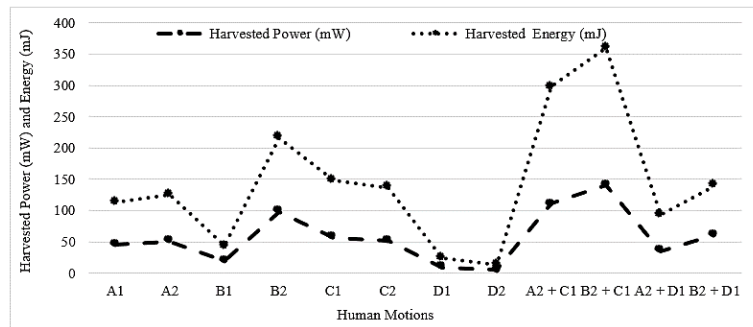


Figure 12. Average harvested power and energy for different human motions in the BM- EHS

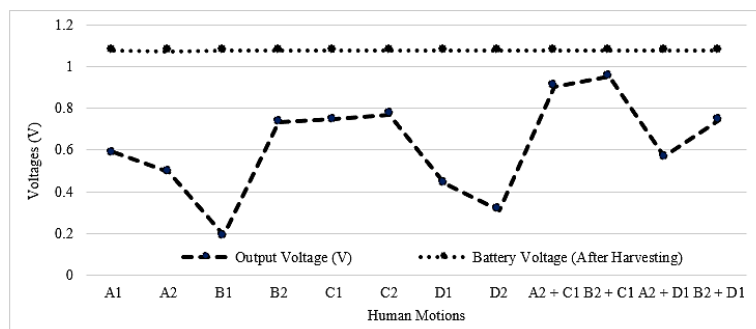


Figure 13. Output voltages and battery voltages for different human motions in the BM- EHS

Table 4. Performance comparison of proposed work with existing EHS

Ref	Vibration source	EHS	Voltage (V)	Power (mW)	Energy (mJ)	Resistive Load
[11]	Knee movement	EM	2	0.092	0.07	2200
[13]	Normal walking	EM	0.8	0.416	NA	10
[18]	Knee-joint	PE	0.1	5.8	6.4	15000
[20]	Human walking	PE	0.9	0.5	5	NA
[21]	Human walking	PE	1.08	6	60	510
[22]	Human Running	EM	0.8	2.28	22.8	25
This work	Normal Walking	PE	0.58	45.9	112.7	100
This work	Knee Movement	EM	0.75	56.6	148.2	100

#### 4. CONCLUSION AND FUTURE WORK

The efficient hybrid biomechanical energy harvesting system is designed from human activities in this manuscript. The hybrid BM-EHS mainly uses two different vibration sources to harvest more power and energy. The PE-EHS and EM-EHS are integrated to form the hybrid BM-EHS. The PE-EHS generates the electric energy from the vibration source of the human walking and jogging activities using the piezoelectric stack and mass-spring-damper model. The EM-EHS generates the electric energy from the vibration source of the human knee and hip movement's activities using angular velocity and DC motor. The boost converter with a control mechanism boosts the desired voltages after integration. The Hybrid BM-EHS is modeled using MATLAB/Simulink. The simulation results, performance metrics, and comparative analysis are realized in detail. The hybrid BH-EMS model provides an average output voltage of 0.79 V and harvests 86.9 mW of power. The hybrid BH-EMS provides better-harvested power in 37.9 % and 64.3 % than the PE-EHS and EM-EHS, respectively. The proposed work is compared with existing similar EHS with better-harvested power and energy improvement. In the future, incorporate the harvested power into the real-time wireless sensor nodes to realize the performance metrics and feasibility.




#### REFERENCES

- [1] A. Khaligh, P. Zeng and C. Zheng, "kinetic energy harvesting using piezoelectric and electromagnetic technologies—state of the art," in *IEEE Transactions on Industrial Electronics*, vol. 57, no. 3, pp. 850-860, March 2010, doi: 10.1109/TIE.2009.2024652.
- [2] L. Qingguo, V. Naing, and J. Maxwell Donelan, "Development of a biomechanical energy harvester," *Journal of neuroengineering and rehabilitation*, vol. 6, no. 1, pp.1-12, 2009, doi: 10.1186/1743-0003-6-22.
- [3] R. Raziell, and A. Shapiro, "Biomechanical energy harvesting from human motion: theory, state of the art, design guidelines, and future directions," *Journal of neuroengineering and rehabilitation*, vol. 8, no. 1, pp. 1-13, 2011, doi: 10.1186/1743-0003-8-22.
- [4] M. Alvaro, B. G. Zapirain, and A. M. Zorrilla, "Gait analysis methods: An overview of wearable and non-wearable systems, highlighting clinical applications," *Sensors*, vol. 14, no. 2, pp. 3362-3394, 2014, doi: 10.3390/s140203362.
- [5] H. Shi, Z. Liu and X. Mei, "Overview of human walking induced energy harvesting technologies and its possibility for walking robotics," *Energies*, vol. 13, no. 1, pp. 1-22, 2020, doi: 10.3390/en13010086.
- [6] Y. Zou, L. Bo, and Z. Li, "Recent progress in human body energy harvesting for the smart bioelectronic system," *Fundamental Research*, vol. 1, no. 3, pp. 364-385, 2021, doi: 10.1016/j.fmre.2021.05.002.
- [7] X. C. Song, Y. Song, M. Han and H. Zhang, "Portable and wearable self-powered systems based on emerging energy harvesting technology," *Microsystems & Nanoengineering*, vol. 7, no. 25, pp. 1-14, 2021, doi: 10.1038/s41378-021-00248-z.
- [8] C. R. Saha, "Modelling theory and applications of the electromagnetic vibrational generator," *In Sustainable Energy Harvesting Technologies: Past, Present, and Future*. Nottingham, UK: Intech, 2011, doi: 10.5772/27236.
- [9] M. Wahbah, M. Alhawari, B. Mohammad, H. Saleh and M. Ismail, "Characterization of human body-based thermal and vibration energy harvesting for wearable devices," *IEEE Journal on Emerging and Selected Topics in Circuits and Systems*, vol. 4, no. 3, pp. 354-363, 2014, doi: 10.1109/JETCAS.2014.2337195.
- [10] D. Dan, and J. Liu, "Hip-mounted electromagnetic generator to harvest energy from human motion," *Frontiers in Energy*, vol. 8, no. 2, pp. 173-181, 2014, doi: 10.1007/s11708-014-0301-2.
- [11] V. Luciano, E. Sardini, M. Serpelloni and G. Baronio, "An energy harvesting converter to power sensorized total human knee prosthesis," *Measurement Science and Technology*, vol. 25, no. 2, pp. 1-12, 2014, doi: 10.1088/0957-0233/25/2/025702.
- [12] S. Khalifa, M. Hassan and A. Seneviratne, "Pervasive self-powered human activity recognition without the accelerometer," *IEEE International Conference on Pervasive Computing and Communications (PerCom)*, 2015, pp. 79-86, doi: 10.1109/PERCOM.2015.7146512.
- [13] M. Niroomand, and H. R. Foroughi, "A rotary electromagnetic microgenerator for energy harvesting from human motions," *Journal of applied research and technology*, vol. 14, no. 4, pp. 259-267, 2016, doi: 10.1016/j.jart.2016.06.002.
- [14] M. Wahbah, M. Alhawari, B. Mohammad, H. Saleh and M. Ismail, "An AC-DC converter for human body-based vibration energy harvesting," *Microelectronics journal*, vol. 55, pp. 1-7, 2016, doi: 10.1016/j.mejo.2016.06.006.
- [15] C. Chen, L. Y. Chau and W. H. Liao, "A knee-mounted biomechanical energy harvester with enhanced efficiency and safety," *Smart Materials and Structures*, vol. 26, no. 6, pp. 1-13, 2017, doi: 10.1088/1361-665.
- [16] A. Ali, N. A. M. Razali, M. Albreem, M. H. Arshad and K. Khalid, "matlab simulink simulation of respiratory effort energy harvester using electromagnetic generator," *Applied Mechanics and Materials, Trans Tech Publications Ltd*, vol. 793, pp. 417-421, 2015, doi: 10.4028/www.scientific.net/AMM.793.417.
- [17] H. Ma and W. H. Liao, "Human gait modeling and analysis using a semi-markov process with ground reaction forces," *IEEE Transactions on Neural Systems and Rehabilitation Engineering*, vol. 25, no. 6, pp. 597-607, 2017, doi: 10.1109/TNSRE.2016.2584923.
- [18] Y. Kuang, Z. Yang and M. Zhu, "Design and characterization of a piezoelectric knee-joint energy harvester with frequency up-conversion through magnetic plucking," *Smart Materials and Structures*, vol. 25, no. 8, pp. 085029, 2016, doi: 10.1088/0964-




- 1726/25/8/085029.
- [19] W. Wang, J. Cao, C. R. Bowen, S. Zhou and J. Lin, "Optimum resistance analysis and experimental verification of nonlinear piezoelectric energy harvesting from human motions," *Energy*, vol. 118, pp. 221-230, 2017, doi: 10.1016/j.energy.2016.12.035.
- [20] R. Kakihara, K. Kariya, Y. Matsushita, T. Yoshimura and N. Fajimura, "Investigation of piezoelectric energy harvesting from human walking," *In Journal of Physics: Conference Series, IOP Publishing*, vol. 1052, no. 1, pp. 012113, 2018, doi: 10.1088/1742-6596/1052/1/012113.
- [21] F. Qian, T. B. Xu and L. Zuo, "Design, optimization, modeling, and testing a piezoelectric footwear energy harvester," *Energy conversion and management*, vol. 171, pp. 1352-1364, 2018, doi: 10.1016/j.enconman.2018.06.069.
- [22] S. Wu, P. C. K. Luk, C. Li, X. Zhao, Z. Jiao and Y. Shang, "An electromagnetic wearable 3-DoF resonance human body motion energy harvester using ferrofluid as a lubricant," *Applied Energy*, vol. 197, pp. 364-374, 2017, doi: 10.1016/j.apenergy.2017.04.006.
- [23] K. Fan, M. Cai, H. Liu and Y. Zhang, "Capturing energy from ultra-low frequency vibrations and human motion through a monostable electromagnetic energy harvester," *Energies*, vol. 169, pp. 356-368, 2019, doi: 10.1016/j.energy.2018.12.053.
- [24] M. A. Halim, M. H. Kabir, H. Cho and J. Y. Park, "A frequency up-converted hybrid energy harvester using transverse impact-driven piezoelectric bimorph for human-limb motion," *Micromachines*, vol. 10, no. 10, no. 701, pp. 1-14, 2019, doi: 10.3390/mi10100701.
- [25] E. Flux, M. M. V. Krogt, P. Cappa, M. Petrarca, K. Desloovere and J. Harlaar, "The human body model versus conventional gait models for kinematic gait analysis in children with cerebral palsy," *Human Movement Science*, vol. 70, 2020, doi: 10.1016/j.humov.2020.102585.
- [26] P. B. Shull and H. Xia, "Modeling and prediction of wearable energy harvesting sliding shoes for metabolic cost and energy rate outside of the lab," *Sensors*, vol. 20, no. 23, pp. 6915, 2020, doi: 10.3390/s20236915.
- [27] T. N. Phan, J. J. Aranda, N. Oelmann and S. Bader, "Design optimization and comparison of cylindrical electromagnetic vibration energy harvesters," *Sensors*, vol. 21, no. 23, pp. 7985, 2021, doi: 10.3390/s21237985.
- [28] A. N. F. Asli and Y. C. Wong, "3.3 V DC output at -16dBm sensitivity and 77% PCE rectifier for RF energy harvesting," *International Journal of Power Electronics and Drive System*, vol. 10, no. 3, pp. 751-758, 2019, doi: 10.11591/ijpeds.v10n3.pp751-758.
- [29] P. T. Tin, D. H. Ha, M. Tran and T. T. Tran, "Jammer against eavesdropper in half-duplex energy harvesting cooperative relaying networks: secrecy outage probability analysis," *International Journal of Power Electronics and Drive Systems*, vol. 11, no. 2, pp. 879-885, 2020, doi: 10.11591/ijpeds.v11.i2.pp879-885.
- [30] K. Kumar *et al.*, "Vision based solar tracking system for efficient energy harvesting," *International Journal of Power Electronics and Drive Systems*, vol. 12, no. 3, pp. 1431-1438, 2021, doi: 10.11591/ijpeds.v12.i3.pp1431-1438.
- [31] T. Gomathi, and M. Shaby, "An efficient and effective energy harvesting system using surface micromachined accelerometer," *International Journal of Power Electronics and Drive Systems*, vol. 12, no. 3, pp. 1068-1074, 2022, doi: 10.11591/ijpeds.v13.i2.pp1068-1074.
- [32] M. Gorlatova, J. Sarik, G. Grebla, M. Cong, I. Kymissis and G. Zussman, "Movers and shakers: kinetic energy harvesting for the internet of things," *IEEE Journal on Selected Areas in Communications*, vol. 33, no. 8, pp. 1624-1639, 2015, doi: 10.1109/JSAC.2015.2391690.
- [33] Y. Xue and L. Jin, "A naturalistic 3D acceleration-based activity dataset & benchmark evaluations," *IEEE International Conference on Systems, Man and Cybernetics*, 2010, pp. 4081-4085, doi: 10.1109/ICSMC.2010.5641790.
- [34] M. G. Kang, W. S. Jung, C. Y. Kang and S. J. Yoon, "Recent progress on PZT based piezoelectric energy harvesting technologies," *In Actuators, Multidisciplinary Digital Publishing Institute*, vol. 5, no. 1, pp. 1-17, 2016, doi: 10.3390/act5010005.
- [35] Permanent Magnet DC Motors, [Online] Available: <https://www.moog.com/content/dam/moog/literature/MCG/moc23series.pdf>. Accessed on March 16, 2022.
- [36] V. Mohankumar and G. V. Jayaramaiah, "Recent progress on biomechanical energy harvesting system from the human body: comprehensive review," *International Journal of Advanced Computer Science and Applications*, vol. 12, no. 7, pp. 184-194, 2021, doi: 10.14569/IJACSA.2021.0120721.
- [37] Mohankumar, V., and G. V. Jayaramaiah, "Simulation of gait based wearable energy harvesting using human movement," *International Journal of Innovative Technology and Exploring Engineering*, vol. 9, no. 4, pp. 1161-1165, 2020, doi: 10.35940/ijitee.c8667.029420.

## BIOGRAPHIES OF AUTHORS



**Mohankumar Venugopal**    is a research scholar pursuing his doctoral degree under Visvesvaraya Technological University, Belagavi at Electronics and Communication Engineering Department, Dr. Ambedkar Institute of Technology, Bangalore. His research interests are Energy Harvesting, Control Systems, and Electronics & Electrical circuits. He can be contacted at email: [phd.mohankumar@gmail.com](mailto:phd.mohankumar@gmail.com).



**Govindanayakanapalya Venkatagiriappa Jayaramaiah**    is currently working as a Professor and Head at the Electrical and Electronics Engineering Department, Dr. Ambedkar Institute of Technology, Bangalore. He has published many papers and written some books. His area of research is Energy harvesting, Power Electronics, and Embedded Systems. He can be contacted at email: [gvjayaram@gmail.com](mailto:gvjayaram@gmail.com).